

Theoretical Study of the Bis-Silylation Reaction of Ethylene Catalyzed by Titanium Dichloride

Yuri Alexeev and Mark S. Gordon*

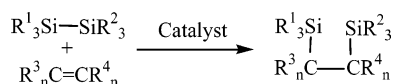
Department of Chemistry, Iowa State University, Ames, Iowa 50011

Received May 7, 2003

Titanium dichloride was investigated as a potential catalyst for the bis-silylation reaction of ethylene with hexachlorodisilane. Ab initio electronic structure calculations at the restricted Hartree–Fock (RHF), density functional (DFT), second-order perturbation (MP2), and couple cluster (CCSD) levels of theory were used to find optimized structures, saddle points, and minimum-energy paths that connect them. The reaction was found to have a net zero barrier at the DFT, MP2, and CCSD levels of theory. Dynamic correlation is found to be important for this reaction.

Introduction

The bis-silylation reaction¹ is an important process for producing bis(silyl) compounds and new C–Si bonds, which can serve as monomers for silicon-containing polymers and silicon carbides. Many of these organo-silicon materials have desirable chemical and physical properties, such as thermal stability and the ability to store and transfer optical and electrical information.^{2,3} However, there is a lack of quantum-chemical calculations for the study of the effect of catalysis on the bis-silylation reaction. Such calculations can potentially lead to the development of new catalysts. In the bis-silylation reaction an Si–Si bond adds across a C–C double or triple bond, in the process breaking a CC π bond and forming two new C–Si bonds. One may write a schematic for the bis-silylation reaction with an alkene as



Experimental and theoretical studies of this reaction in the absence of a catalyst suggest that the reaction has a high activation barrier. For example, the predicted barrier height for the addition of disilane to ethylene to form 1,2-disilylethane is predicted to be approximately 50 kcal/mol, using second-order perturbation theory.⁴ Indeed, this high barrier seems to be insensitive to the level of theory employed. This suggests, as is well-known to experimentalists, that a catalyst is required to make this reaction practical, certainly in any industrial sense.

A number of bis-silylation catalysts have been employed since 1972, when Okinoshima et al. carried out

the first successful double silylation of 1,3-butadienes using Ni phosphine complexes as catalysts.⁵ Later Okinoshima,⁶ Watanabe,^{7–9} and others discovered that Rh, Ni, Pt, and Pd phosphine complexes can be used to add substituted disilanes across various unsaturated acetylene and ethylene derivatives. It was found that complexes such as M(PPh₃)₄ and MCl₂(PPh₃)₂, where M is Pt or Pd, are the most efficient catalysts. Recently Bottoni et al.¹⁰ used density functional theory (DFT) with the B3LYP functional¹¹ to study the bis-silylation reaction of acetylene with disilane, H₃Si–SiH₃, in the presence of Pd(PH₃)₂. Pd(PH₃)₂ was used to emulate Pd(PPh₃)₂, PdCl₂(PEt₃)₂, and other catalysts often used in experimental studies. The net reaction barrier was predicted to be 18 kcal/mol.

A theoretical study of Pt(PH₃)₂-catalyzed bis-silylation and hydrosilylation (using the Chalk–Harrod and modified Chalk–Harrod mechanisms) of alkenes was recently performed by Sakaki et al.^{12,13} These authors used second-order perturbation theory (MP2),¹⁴ fourth-order perturbation theory (MP4SDQ),¹⁵ and doubles coupled cluster theory (CCD)¹⁶ to study the reactions. The net reaction barrier is predicted to be 19 kcal/mol in the bis-silylation reaction and 5 kcal/mol in the Chalk–Harrod mechanism of the hydrosilylation reaction. Thus, the two theoretical studies agree that, even in the presence of a catalyst, the energy barrier is still nontrivial.

(5) Okinoshima, H.; Yamamoto, K.; Kumada, M. *J. Am. Chem. Soc.* **1972**, *94*, 9263.

(6) Okinoshima, H.; Yamamoto, K.; Kumada, M. *J. Organomet. Chem.* **1975**, *86*, C27.

(7) Watanabe, H.; Kobayashi, M.; Saito, M.; Nagai, Y. *J. Organomet. Chem.* **1981**, *149*, 216.

(8) Watanabe, H.; Saito, M.; Sutou, N.; Kishimoto, K.; Inose, J.; Nagai, Y. *J. Organomet. Chem.* **1982**, *225*, 343.

(9) Watanabe, H.; Kitahara, T.; Motegi, T.; Nagai, Y. *J. Organomet. Chem.* **1977**, *215*, 139.

(10) Bottoni, A.; Higuero, A. P.; Miscione, G. P. *J. Am. Chem. Soc.* **2002**, *124*, 5506.

(11) Koch, W.; Holthausen, M. C. *A Chemist's Guide to Density Functional Theory*; Wiley: Weinheim, Germany, 2000.

(12) Sakaki, S.; Ogawa, M.; Musashi, Y. *J. Organomet. Chem.* **1997**, *535*, 25.

(13) Sakaki, S.; Mizoe, N.; Sugimoto, M.; Musashi, Y. *Coord. Chem. Rev.* **1999**, *190–192*, 933.

(14) Moler, C.; Plesset, M. S. *Phys. Rev.* **1934**, *46*, 618.

(15) Cramer, C. J. *Essentials of Computational Chemistry*; Wiley: New York, 2000.

(16) Crawford, T. D.; Schaefer, H. F., III. *Rev. Comput. Chem.* **1996**, *14*, 33.

* Corresponding author.

(1) Jones, R. G.; Ando, W.; Chojnowski, J. *Silicon-Containing Polymers: The Science and Technology of Their Synthesis and Applications*; Kluwer Academic: Dordrecht, The Netherlands, 2000.

(2) (a) Lee, H. H. *Fundamentals of Microelectronic Processing*; McGraw-Hill: New York, 1990. (b) Mort, J.; Jansen, F. *Plasma Deposited Thin Films*; CRC Press: Boca Raton, FL, 1986. (c) Sueta, T.; Okoshi, T. *Ultrafast and Ultra-Parallel Optoelectronics*; Wiley: Tokyo, 1995. (d) Prasad, P. N.; Ulrich, D. R. *Nonlinear Optical and Electroactive Polymers*; Plenum Press: New York, 1988.

(3) (a) Bradley, D. C. *Chem. Rev.* **1989**, *89*, 1317. (b) Hench, L. L.; West, J. K. *Chem. Rev.* **1990**, *90*, 33.

(4) Raaij, F.; Gordon, M. S. *J. Phys. Chem. A* **1998**, *102*, 4666.

It is well-known that complexes of early transition metals, such as Ti and Zr, exhibit catalytic properties. In the Ziegler–Natta polymerization reaction, the commonly used catalysts are MCl_4-ALR_3 and MR_2 , where M is Ti or Zr.¹⁷ The first step in the currently accepted mechanism is formation of a metal–alkyl–olefin complex. The addition of $Cl_2TiCH_3^+$ to C_2H_4 was studied recently by Bernardi et al.¹⁸ with DFT using the B3LYP functional. The reaction is predicted to require no net barrier. A π -complex intermediate that is found to be lower in energy than the reactants by 38 kcal/mol apparently drives this catalyzed reaction by providing an initially large exothermicity.

Titanocene- ($TiCp_2$, where Cp = cyclopentadienyl) and zirconocene-based catalysts ($ZrCp_2$) were recently reported to be efficient catalysts for double silylation by Terao et al.¹⁹ and Harrod et al. In particular, double silylation of isoprene with chlorotriethylsilane proceeds with 91% yield at 0 °C in the presence of Cp_2TiCl_2 and $BuMgCl$ in THF solution. The double silylation of *p*-chlorostyrene by $Me_2PhSiCl$ in the presence of $BuMgCl$ and Cp_2TiCl_2 in THF solution under the same conditions gives a 72% yield.

In the works of both Harrod et al.²⁰ and (more recently) Terao et al.,¹⁹ it was found that derivatives of $TiCp_2$ such as Cp_2TiCl_2 are efficient catalysts for silylation and double silylation of various unsaturated hydrocarbons. It is postulated that $TiCp_2$ is the active catalyst. The role of $TiCp_2$ has been studied in great detail by Harrod et al.²⁰

Inspired by the Ziegler–Natta reaction, Bode, Day, and Gordon²¹ investigated the possibility that divalent Ti compounds might also function as effective catalysts for the hydrosilylation reaction. Because of the size of $TiCp_2$, these authors employed the model divalent Ti catalysts TiH_2 and $TiCl_2$, as well as $TiCp_2$, to determine if the former compounds are predicted to be as effective as the actual $TiCp_2$ catalyst.²⁶ They employed several levels of theory, including second-order perturbation theory (MP2) and coupled cluster theory (CCSD(T)). The key results with respect to the present effort are that (a) the two correlation methods MP2 and CCSD(T) give very similar energy predictions and (b) the catalytic effect of $TiCl_2$ is very similar to that of $TiCp_2$. The former observation suggests that MP2 is a reliable method to use for larger systems. The latter point is critical, since it means that one can do more tractable calculations on the model $TiCl_2$, with some assurance that the results for $TiCp_2$ will be similar. For both MP2 and CCSD(T), the initial step in the hydrosilylation reaction is highly exothermic, thereby driving the reaction sufficiently downhill that there is no net barrier along the entire reaction path. This suggests that the driving force in

the catalytic activity is similar in the Ziegler–Natta and hydrosilylation reactions—the initial formation of a very stable intermediate.

The purpose of the present work is to present ab initio calculations on possible mechanisms for the catalyzed bis-silylation reaction. On the basis of the discussion in the previous paragraph, $TiCl_2$ is used as a model catalyst for the bis-silylation reaction of ethylene with hexachlorodisilane. This choice of reactants allows us to study this reaction at reliable levels of theory without compromising accuracy, and, as noted above, $TiCl_2$ is expected to reliably mimic $TiCp_2$. Since $TiCp_2$ is thought to be the active industrial catalyst for producing organosilicon polymers on the basis of the results of Harrod et al.²⁰ and the recent report by Terao et al.,¹⁹ it is reasonable to consider $TiCl_2$ as a viable model for the efficient catalyst $TiCp_2$.

Computational Methods

All calculations performed for this paper were carried out using the GAMESS program,²² and figures were generated using the MacMolPlt program.²³ The basis set used in the calculations was the SBKJC effective core potential (ECP) basis²⁴ on Si, Cl, and Ti. One d-type polarization function was added on each Si and Cl atom.²⁵ The H and C atom basis used was 6-31G (d,p). This basis set was compared previously²⁶ with an all-electron triple- ζ plus polarization basis set. It was found that the difference in relative energies between these is less than 0.5 kcal/mol, consistent with the present work.

The RHF, DFT, MP2, and CCSD methods were used to study the bis-silylation reaction. Preliminary geometry calculations were carried out using RHF. These geometries were then used as starting geometries for the MP2 calculations. DFT and CCSD calculations were carried out at selected transition states with the highest energy barriers. These methods predict results that are similar to those from MP2. Only the RHF method predicts a nonzero net barrier.

All geometries and energies for reactants, products, and all stationary points on the reaction path presented in this paper are at the MP2 level of theory. Each stationary point was confirmed by computing the Hessian (matrix of second derivatives of energy). The diagonalized Hessian provides harmonic normal modes and corresponding vibrational frequencies. Transition states and minima are indicated by one and no imaginary mode, respectively. The calculated frequencies were also used to compute zero-point vibrational energies (ZPE).

Finally, each confirmed transition state has been connected to reactants and products using the Gonzales–Schlegel second-order intrinsic reaction coordinate (IRC) method with a step size of 0.3 amu^{1/2} bohr.

Results and Discussion

The previous studies established that dynamic correlation is important for reactions in which Ti is a catalyst; therefore, the MP2 and CCSD methods were employed. MP2 natural orbital occupation numbers (NOONs) were calculated and inspected at each stationary point. The largest observed deviation from the HF

(17) (a) Novaro, O.; Blaisten-Barojas, E.; Clementi, E.; Giunchi, G.; Ruiz-Vizcaya, M. E. *J. Chem. Phys.* **1978**, *68*, 2337. (b) Kawamura-Kuribayashi, H.; Koga, N.; Morokuma, K. *J. Am. Chem. Soc.* **1992**, *114*, 2359. (c) Meier, R. J.; van Doremale, G. H. J.; Iarlori, S.; Buda, F. *J. Am. Chem. Soc.* **1994**, *116*, 7274.

(18) Bernardi, F.; Bottoni, A.; Miscione, G. P. *Organometallics* **1998**, *17*, 16.

(19) (a) Terao, J.; Kambe, N. *J. Synth. Org. Chem. Jpn.* **2001**, *59*, 1044. (b) Terao, J.; Kambe, N.; Sonoda, N. *Tetrahedron Lett.* **1998**, *39*, 9697. (c) Terao, J.; Torii, K.; Saito, K.; Kambe, N.; Baba, A.; Sonoda, N. *Angew. Chem., Int. Ed. Engl.* **1998**, *37*, 2653.

(20) Harrod, J. F.; Ziegler, T.; Tschinke, V. *Organometallics* **1990**, *9*, 897.

(21) Bode, B. M.; Day, P. N.; Gordon, M. S. *J. Am. Chem. Soc.* **1998**, *120*, 1552.

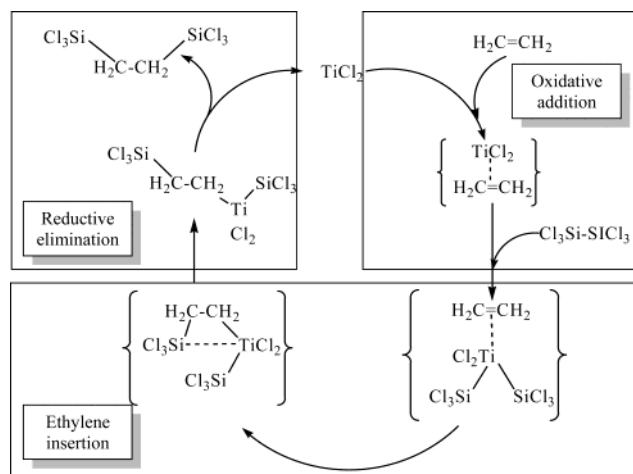
(22) Schmidt, M. W.; Baldridge, K. K.; Boatz, J. A.; Elbert, S. T.; Gordon, M. S.; Jensen, J. J.; Koseki, S.; Matsunaga, N.; Nguyen, K. A.; Su, S.; Windus, T. L.; Dupuis, M.; Montgomery, J. A. *J. Comput. Chem.* **1993**, *14*, 1347.

(23) Bode, B. M.; Gordon, M. S. *J. Mol. Graphics* **1999**, *16*, 133.

(24) (a) For Si and Cl: Stevens, W. J.; Basch, H.; Krauss, M. *J. Chem. Phys.* **1984**, *81*, 6026. (b) For Ti: Stevens, W. J.; Basch, H.; Krauss, M.; Jasien, P. *Can. J. Chem.* **1992**, *70*, 612.

(25) The exponents used are as follows: Si, $\zeta_d = 0.364$; Cl, $\zeta_d = 0.566$.

(26) Bode, B.; Gordon, M. S. *Theor. Chem. Acc.* **1998**, *102*(1–6), 366.

Scheme 1. Catalytic Cycle for Double Silylation of Ethylene with Hexachlorodisilane


values of 2.0 and 0.0 for occupied and virtual orbitals, respectively, is 0.08, suggesting that there is little multiconfigurational character in the wave function.²⁷ The MP2 geometries and energies are presented in all figures and tables.

In the commonly accepted mechanism for bis-silylation of alkenes and alkynes^{28–30} the first step is oxidative addition of the catalyst to the disilane; then the alkene or alkyne is inserted into the metal–silyl bond. The final stage is reductive elimination and the regeneration of the catalyst. In the experiments no intermediates have been detected in the oxidative addition of Pt(0) to disilane, presumably confirming the first step³¹ in this mechanism. On the basis of the current calculation with $TiCl_2$, an alternative mechanism is presented in Scheme 1, in which the first step is oxidative addition of the catalyst to the ethylene, not the disilane, to form an initial complex. The complex interacts with disilane. Subsequently, ethylene is inserted into the Ti–Si bond to form product after reductive elimination of the $TiCl_2$ catalyst.

The overall reaction path energetics are demonstrated in Figure 1. The reactants are labeled as R, minima as MX (where X is an integer number), transition states as TSX, and products as P. Minima M3 and M4, M5 and M6, M7 and M8, M8 and M9, and M9 and M10 were connected by using linear least motion paths and constrained optimization techniques. The highest point on a constrained optimization path is an upper bound to the energy barrier for that path. Each step will be discussed in detail in the following sections. The relative MP2 energies presented in Figure 1 do not include vibrational ZPE corrections. In the first column of Table 1 relative MP2 electronic energies corresponding to the data in Figure 1 are listed. ZPE-corrected relative energies are presented in the last column of Table 1.

(27) Gordon, M. S.; Schmidt, M. W.; Chaban, G. M.; Glaesemann, K. R.; Stevens, W. J.; Gonzalez, C. *J. Chem. Phys.* **1999**, *110*, 4199.

(28) Hayashi, T.; Kobayashi, T.; Kawamoto, A. M.; Yamashita, H.; Tanaka, M. *Organometallics* **1990**, *9*, 280.

(29) Murakami, M.; Yoshida, T.; Ito, Y. *Organometallics* **1994**, *13*, 2900.

(30) Sakaki, S.; Ogawa, M.; Musashi, Y. *J. Organomet. Chem.* **1997**, *535*, 25.

(31) Michalczyk, M. J.; Calabrese, J. C.; Recatto, C. A.; Fink, M. J. *J. Am. Chem. Soc.* **1992**, *114*(20), 7955. Heyn, R. H.; Tilley, T. D. *J. Am. Chem. Soc.* **1992**, *114*(5), 1917.

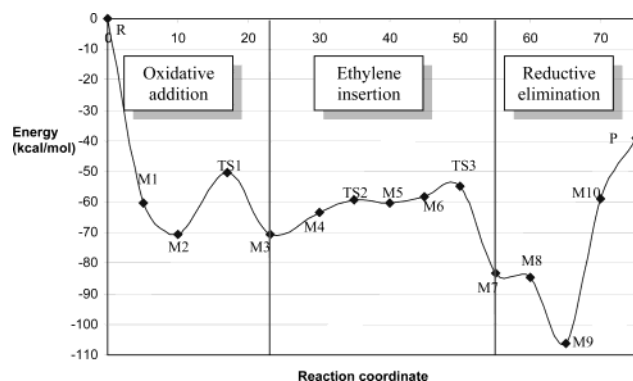


Figure 1. Minimum energy reaction path.

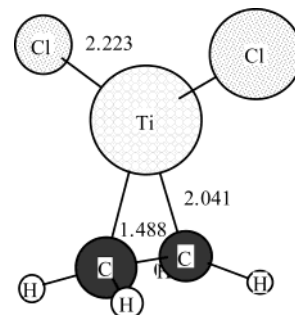


Figure 2. $TiCl_2-C_2H_2$ complex.

Table 1. MP2 Relative Energies with ZPE Corrections in kcal/mol

structure	relative energy		structure	relative energy		
	MP2	MP2 + ZPE		MP2	MP2 + ZPE	
Oxidative Addition						
R	0	0	TS1	-50.5	-48.2	
M1	-60.5	-59.6	M3	-70.5	-67.9	
M2	-70.6	-68.9				
Ethylene Insertion						
M4	-63.3	-60.9	M6	-58.4	-55.9	
TS2	-59.4	-57.1	TS3	-54.7	-52.3	
M5	-60.1	-57.9	M7	-83.3	-80.7	
Reductive Elimination						
M8	-84.6	-82.2	M10	-59.0	-55.4	
M9	-106.4	-102.9	P	-39.1	-36.2	

In the following sections we will discuss in detail the potential energy surface (PES) of the proposed mechanism: (1) oxidative addition, (2) ethylene insertion into the Ti–Si bond, and (3) reductive elimination. For each step a figure with detailed geometry information for the stationary points is presented, with bond lengths shown in angstroms. For transition states the magnitude of the imaginary frequency is included.

The MP2 total energies and MP2 total ZPE corrected energies for each stationary point in Figure 1 and Table 1 are available in Table S1 of the Supporting Information. The Cartesian coordinates of all geometries can be found in Table S2.

1. Oxidative Addition. Two scenarios have been investigated. The catalyst $TiCl_2$ can attack the C–C bond first, as shown in Figure 2, or $TiCl_2$ can initially attack the Si–Si bond, as shown in Figure 3.

The optimized structures in Figures 2 and 3 have a large difference in energy relative to the energy of the initial reactants: $TiCl_2-C_2H_4$ is lower in energy than $TiCl_2-Si_2Cl_6$ by 42.7 kcal/mol, as can be seen in Table

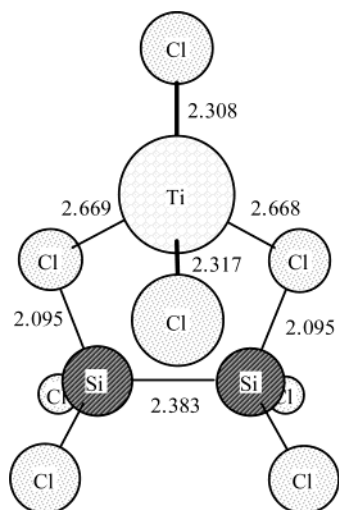


Figure 3. $\text{TiCl}_2\text{-Si}_2\text{Cl}_6$ complex.

2. In the first mechanism, the $\text{TiCl}_2\text{-C}_2\text{H}_4$ complex shown in Figure 2 reacts with Si_2Cl_6 in a series of steps ultimately leading to products. In the second mechanism, the $\text{TiCl}_2\text{-Si}_2\text{Cl}_6$ complex shown in Figure 3 reacts with C_2H_4 in a series of steps that converges to the minimum M2 in Figure 4. Therefore, the second mechanism leads to the same reaction path as the first

Table 2. MP2 Relative Energies with ZPE Corrections in kcal/mol

structure	relative energy	
	MP2	MP2 + MP2 ZPE
reactants	0	0
$\text{TiCl}_2\text{-C}_2\text{H}_4 + \text{Si}_2\text{Cl}_6$	-60.5	-59.6
$\text{TiCl}_2\text{-Si}_2\text{Cl}_6 + \text{C}_2\text{H}_4$	-17.8	-17.1

mechanism. Since (a) the first mechanism leads to a much lower energy initial intermediate M1, (b) both mechanisms proceed through the M2 intermediate shown in Figure 4, and (c) the highest point on each path is lower in energy than the separated reactants, only the first mechanism is presented in detail here (see Scheme 1 and Figure 4). Of course TiCl_2 can attack the $\text{SiCl}_3\text{-SiCl}_3$ bond from different angles, but an MP2 analysis of the relative energies still suggests that the preferred mechanism is initial attack on ethylene.

The MP2 structures for the oxidative addition step are presented in Figure 4. After TiCl_2 forms a complex with ethylene in M1, Ti in this complex interacts with a Cl from disilane, leading to the new intermediate M2. The transition state TS1 connects M2 with M3, in which Ti has broken the hexachlorodisilane Si-Si bond. TS1 and M3 both have C_{2v} symmetry, but M2 has C_1 symmetry. Therefore, a bifurcation³² occurs along the reaction path that connects TS1 with M2, since the

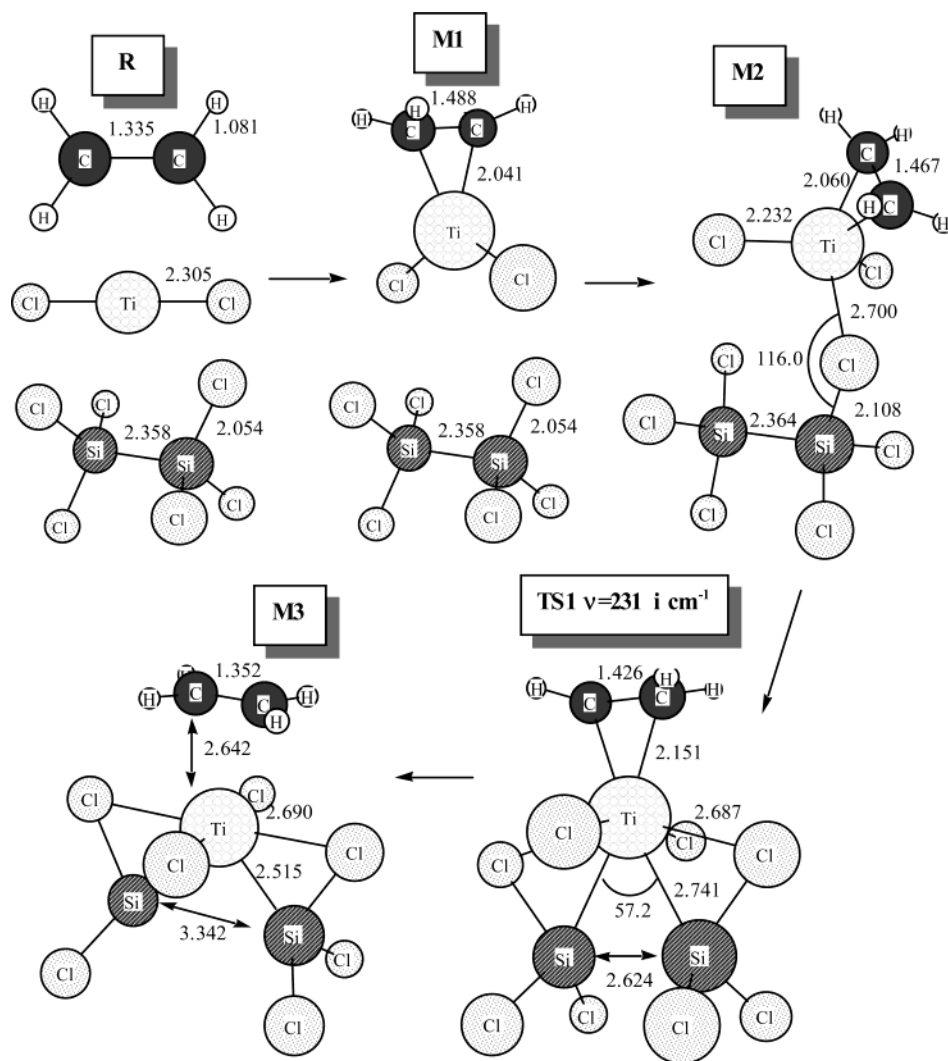


Figure 4. Oxidative addition.

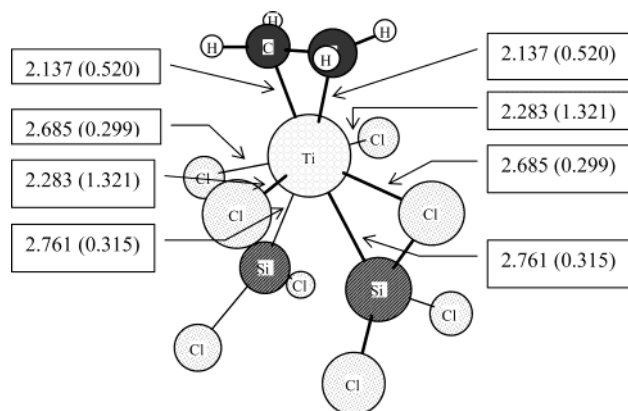


Figure 5. Transition state 1 (TS1) with bond distanced in Å (bond orders given in parentheses).

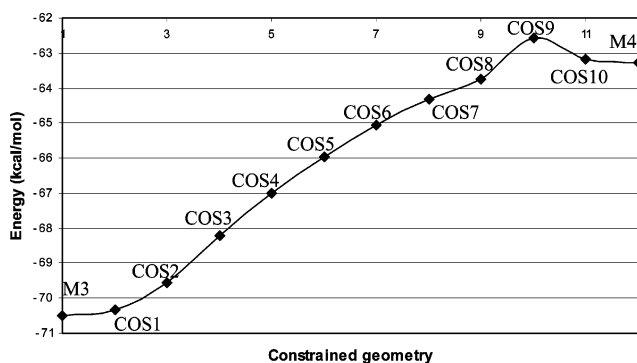


Figure 6. Constrained optimization path connecting M3 and M4. COSX denotes constrained optimized structures.

valley–ridge inflection point does not coincide with the transition state TS1. The valley–ridge inflection point was found by first performing a series of Hessian calculations. Then, the imaginary mode was offset by 5% and the IRC run was resumed to find the correct minimum M2. TS1 is the highest point on the minimum energy reaction path. On the basis of bond and valence analysis, Ti in TS1 forms eight partial bonds with bond orders varying from 0.3 to 1.3 (Figure 5). Ti forms strong bonds with two chlorines perpendicular to the Si–Ti–Si plane and with the two carbon atoms.

It is interesting to track the C–C bond length changes in the oxidative addition step. In M1 the C–C length has single-bond character after ethylene has interacted with Ti. Later, after Ti has inserted into the Si–Si bond in M3, the C–C distance has decreased back to a distance very close to that in ethylene.

The activation energy leading from M2 to TS1 to M3 is 20 kcal/mol. This is the largest activation energy along the reaction path. The energy of M2 relative to M3 is 1 kcal/mol after the ZPE correction is applied. It was expected that the Ti insertion into the Si–Si bond would have one of the highest activation energies, but it is still 50 kcal/mol below the energy of the reactants.

2. Ethylene Insertion. The first step in the ethylene insertion (see Scheme 1 and Figure 7) is to position the ethylene molecule just above the Ti–Si bond. The potential energy surface in this region is shallow, because the ethylene molecule can essentially undergo free rotation. Therefore, a linear least motion path³³ and constrained optimization techniques³⁴ were employed to connect the minimum M3 with M4 and M5 with M6 (Scheme 1).

An example of how the constrained optimization technique is employed is shown in Figure 6. The energies of 10 constrained optimized structures from COS1 to COS10 connecting the M3 and M4 minima are plotted. The estimated activation barrier for the reaction at COS9 is 7.9 kcal/mol, excluding the ZPE correction. The difference in energy between M3 and M4 is 7.0 kcal/mol. The geometry and location of COS9 on the PES is consistent with the Hammond postulate: COS9 is structurally close to the minimum M4, which is 7.2 kcal/mol higher in energy than M3. The primary effect of the M3 → M4 rearrangement is to move one ethylene C closer to its Si partner. The M4 and M5 minima in Figure 7 are connected via a transition state TS2 with an activation energy of 4 kcal/mol (3 kcal/mol with the ZPE correction). In M5 a rotation about the Ti–Si bond has occurred, in order to further facilitate the formation of the new C–Si bond. Minima M5 and M6 are connected in a manner similar to that used to connect minima M3 and M4, with an activation barrier of approximately 2 kcal/mol.

In the second part of the ethylene insertion reaction (Figure 7), the transition state TS3 connects minima M6 and M7. The barrier height of this reaction is 3.6 kcal/mol. TS3 is the second highest stationary point. The energies of M6 and M7 relative to reactants are –55.9 and –80.7, respectively.

In M6, the C–C bond is already slightly stretched from 1.335 Å in ethylene to 1.359 Å, and the Ti–Si bond is stretched from 2.515 Å in M3 to 2.753 Å in M6. In transition state TS3, a four-membered ring is formed that consists of Ti, two carbons, and Si. The Ti–Si bond is stretched even further to 2.949 Å in TS3. The four-membered ring is opened via breaking a Ti–Si bond to give the minimum M7. In M7 the Ti–Si bond is broken, since the distance is 3.680 Å, and a C–Si bond is finally formed. Therefore, M7 is the first time the Si–Ti–C–C–Si chain is formed.

3. Reductive Elimination. The final phase in the overall mechanism is the regeneration of the catalyst and formation of the final product. The geometries of all stationary points in this step are shown in Figure 8. The reaction proceeds in four steps. In the first step, the $SiCl_3$ group attached to $TiCl_2$ moves into the staggered position (M8) relative to the Ti–C bond. Since internal rotations usually require little activation energy, the constrained optimization technique was utilized to connect M7 and M8. The estimated activation energy required to connect minima M7 and M8 is 3.4 kcal/mol. The energies of M7 and M8 relative to the reactants are –80.7 and –82.2, respectively, including the ZPE correction.

In the next step, M8 → M9, Ti and Si interchange their positions. M9 is the first species in which the Ti–Si–C–C–Si linkage appears. To connect minima M8 and M9, the constrained optimization technique was used. The estimated barrier height is 5.7 kcal/mol. The intermediate M9 is the global minimum on the reaction path. Including the ZPE correction, M9 is 102.9 kcal/mol below the energy of separated reactants.

(32) Ruedenberg, K.; Valtazanos, P. *Theor. Chim. Acta* **1986**, *69*, 281.

(33) Pechukas, P. *J. Chem. Phys.* **1976**, *64*, 1516.

(34) Baker, J.; Kessi, A.; Delley, B. *J. Chem. Phys.* **1996**, *105*, 192.

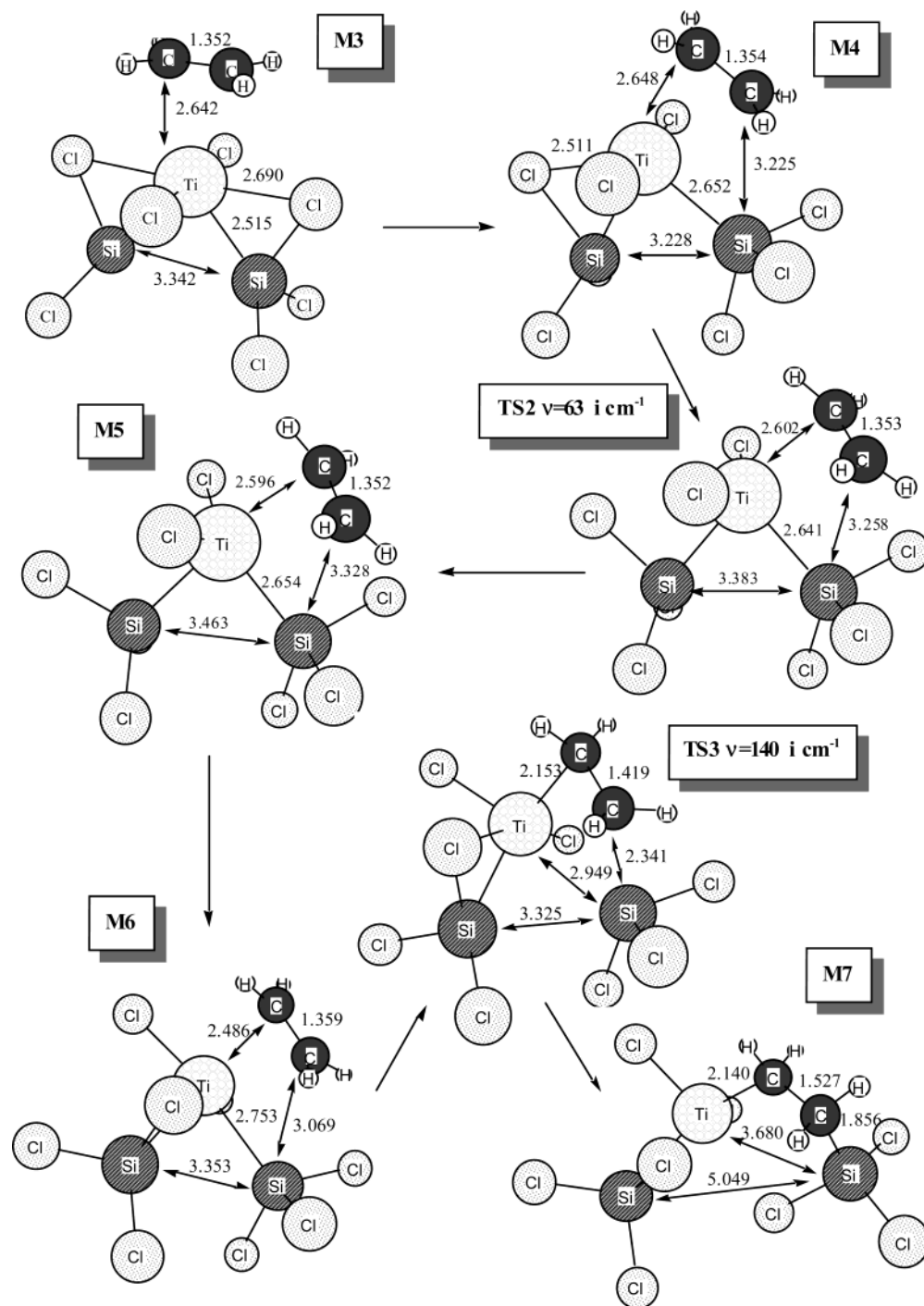


Figure 7. Ethylene insertion.

In the last two steps the catalyst is regenerated. First, one Cl atom on the TiCl₂ group migrates to a Si atom. Then, the new minimum M10 is formed, in which Ti, Si, and two chlorines form a four-membered ring. Two chlorines are shared between Ti and Si. Note that Ti is not connected to either Si in M10. The reaction M9 → M10 is endothermic, with the top of the constrained optimization path being 2.9 kcal/mol above M10. The last step removes the catalyst from the system. No net transition state is expected for this step. The reverse reaction for adding TiCl₂ to product proceeds readily without any barrier. The product is the *cis* conformer of 1,2-bis(chlorosilyl)ethane. The energies of M10 and the product P relative to reactants are -55.4 and -36.2 kcal/mol, respectively, with the ZPE correction.

Conclusions

This paper presents an analysis of the possibility that divalent Ti compounds, using TiCl₂ as a model for TiCp₂, might be as effective catalysts for the bis-silylation reaction as they apparently are for the Ziegler-Natta and hydrosilylation reactions. The net bis-silylation reaction is predicted to be a highly exothermic barrierless process. The products are found to be 36.2 kcal/mol lower in energy than the combined energies of the separated reactants after the MP2 energies are corrected for vibrational zero point effects. Whereas the barrier for this reaction in the absence of a catalyst is ~50 kcal/mol, the presence of the TiCl₂ catalyst reduces this barrier to zero. This may be compared with previous

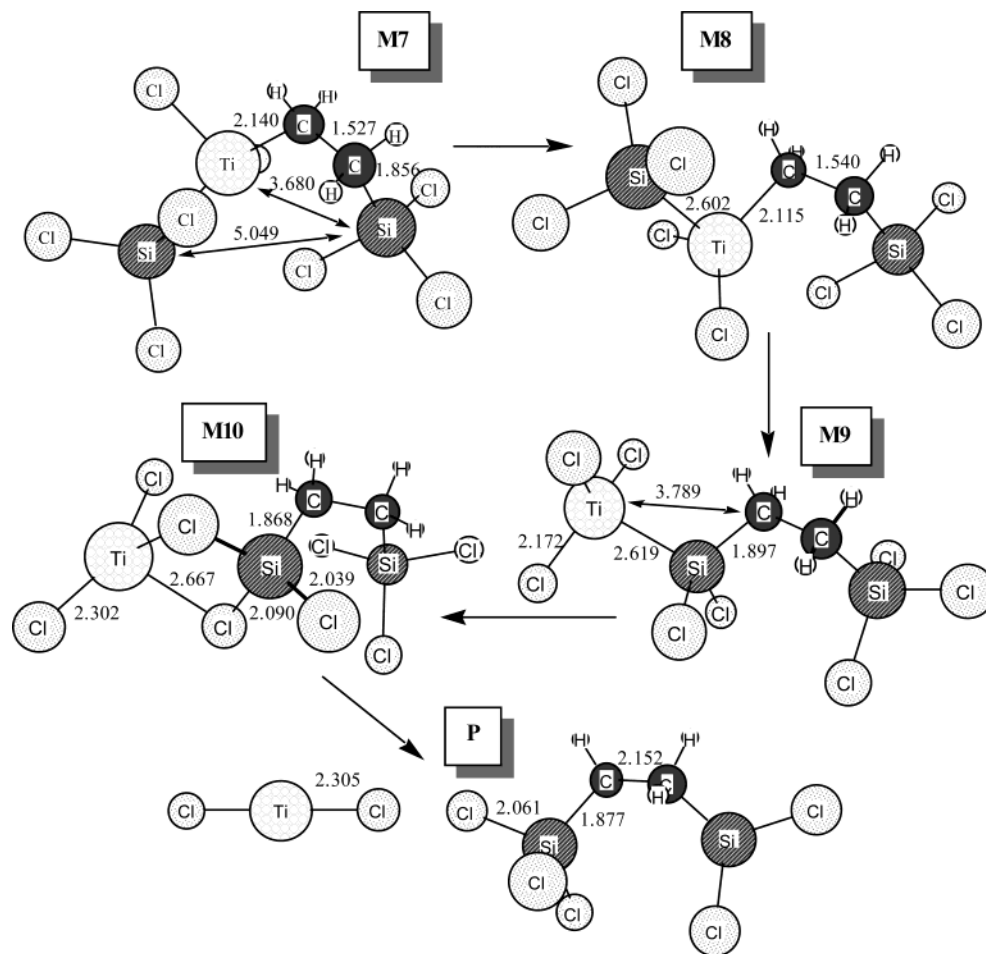


Figure 8. Reductive elimination.

calculations, in which complexes of group X metals reduce the barrier to only $\sim 18\text{--}20$ kcal/mol.^{10–13} Thus, in this sense, divalent Ti may be a more effective catalyst for the bis-silylation reaction.

The first step in the predicted mechanism is an interaction of TiCl_2 with ethylene to form an intermediate that is 60 kcal/mol below the energy of the reactants. This is the driving force for the entire reaction. After that, TiCl_2 easily cleaves the Si–Si bond with modest a 20 kcal/mol activation energy. The transition state for this step is the highest point except products for the entire reaction, and it is still 50 kcal/mol below the energy of the reactants. As discussed in several recent papers,^{35–37} Ti is an electron-deficient atom, in much the same manner as B. This means Ti readily forms additional bonds beyond the “usual” four. As noted previously for the hydrosilylation reaction, this makes divalent Ti a particularly effective catalyst, since the initial steps in which Ti binds to one of the reactants is especially facile with a large energy decrease. This energy decrease is sufficient to ensure that the activation barriers for all subsequent steps are well below the energy of the reactants. Consequently, the reaction proceeds easily. It is critical to include dynamic correlation (via MP2) in the calculation, since many of the relative energies and even geometries are in serious error at the Hartree–Fock level of theory. In particular,

RHF calculations incorrectly predict that the net barrier for the catalyzed reaction is 50 kcal/mol.

Because the calculations reported here focus on the potential energy surface for the mechanism by which the bis-silylation reaction proceeds, the dynamics and kinetics for the reaction are not accounted for. In this regard, it is important to note that the presence of the deep intermediate minimum M9 does not suggest that reaction will stop there, because there is enough energy (~ 40 kcal/mol) to push the reaction toward products. In the actual reaction all minima are in equilibrium with each other. Therefore, the removal of the catalyst as product ensures continuous flow of the reaction.

Acknowledgment. The calculations in this work were performed on an IBM workstation cluster made possible by grants from IBM in the form of a Shared University Research grant, the Department of Energy, and a DURIP grant from the Air Force Office of Scientific Research. The research reported here was made possible by a grant from the Air Force Office of Scientific Research.

Supporting Information Available: MP2 total energies with ZPE corrections (Table S1) and Cartesian coordinates of each stationary point (Table S2). This material is available free of charge via the Internet at <http://pubs.acs.org>.

(35) Webb, S. P.; Gordon, M. S. *J. Am. Chem. Soc.* **1999**, *121*, 2552.

(36) Webb, S. P.; Gordon, M. S. *J. Am. Chem. Soc.* **1998**, *120*, 3846.

(37) Webb, S. P.; Gordon, M. S. *J. Am. Chem. Soc.* **1995**, *117*, 7195.